

Interface-resolved simulations of small inertial particles in turbulent channel flow

Pedro Costa^{1†}, Luca Brandt¹ and Francesco Picano²

¹Linné FLOW Centre and SeRC (Swedish e-Science Research Centre), KTH Mechanics, SE-100 44 Stockholm, Sweden

²Department of Industrial Engineering, University of Padova, Via Venezia 1, 35131 Padova, Italy

(Received xx; revised xx; accepted xx)

We present a direct comparison between interface-resolved and one-way-coupled point-particle direct numerical simulations (DNS) of gravity-free turbulent channel flow of small inertial particles, with high particle-to-fluid density ratio and diameter of about 3 viscous units. The most dilute flow considered, solid volume fraction $O(10^{-5})$, shows the particle feedback on the flow to be negligible, whereas differences with respect to the unladen case, noteworthy a drag increase of 10%, are found for volume fraction $O(10^{-4})$. This is attributed to a dense layer of particles at the wall, caused by turbophoresis, flowing with large particle-to-fluid apparent slip velocity. The most dilute case is therefore taken as the benchmark for accessing the validity of a widely-used point-particle model, where the particle dynamics results from inertial and non-linear drag forces. In the bulk of the channel, the first and second-order moments of the particle velocity from the point-particle DNS agree well with those from the interface-resolved DNS. Close to the wall, however, most of the statistics show major qualitative differences. We show that this difference is due to a mechanism for wall-detachment caused by short-range particle-wall interactions that is not reproduced by the point-particle model.

1. Introduction

Turbulent flows laden with small inertial particles are found in many environmental and industrial contexts. These flows are inherently chaotic and multi-scale, with the inter-phase coupling categorized by relevance of the dispersed phase on the overall dynamics (Elghobashi 1994). The so-called *one-way* coupling regime corresponds to low volume and mass fractions of the solid phase, when particle-fluid interactions are negligible, and particle-particle interactions unlikely. Increasing the solid mass fraction while keeping the volume fraction at the same order of magnitude results in a regime where the overall particle load becomes high enough to modulate the turbulent flow, while particle-particle interactions remain negligible – *two-way* coupling. Finally, further increasing the volume fraction results in a regime where particle-particle interactions are also important – *four-way* coupling regime. From a modelling perspective, another important distinction concerns the particle size. When the ratio between the particle size and the Kolmogorov scale is smaller than one, the term *point-particle* is used, and particle-fluid coupling is considered to take place at a single point. Conversely, when the size ratio is large, the particles are termed *finite-sized* (Balachandar & Eaton 2010).

Particle-laden turbulence in the one-way coupling and point-particle limit has been subject of numerous studies throughout the last decades (see e.g. Toschi & Bodenschatz

† Email address for correspondence: pedrosc@mech.kth.se

2009; Balachandar & Eaton 2010, for recent reviews). In these cases, it is assumed that the local properties of an *undisturbed* flow at the particle position drive the dispersed-phase dynamics (Maxey & Riley 1983; Gatignol 1983). For relatively high particle-to-fluid density ratios, the particle dynamics is often simplified to a balance between particle inertial and drag forces, where the latter is a function of the so-called particle-to-fluid slip velocity. Under these conditions, particles display preferential clustering even in homogeneous and isotropic flows (Toschi & Bodenschatz 2009). When the flow is inhomogeneous, particles tend to migrate from regions of high to low turbulence intensity due to turbophoresis (Reeks 1983). In turbulent wall-bounded flows in particular, the particle distribution is driven by the interplay between small-scale clustering, turbophoresis, and the interaction between the particles and near-wall turbulence structures (Soldati & Marchioli 2009; Sardina *et al.* 2012). When the system reaches a statistical equilibrium, particles tend to accumulate in the low-speed regions near the wall, resulting in a very inhomogeneous local particle concentration; see e.g. Fessler *et al.* (1994); Uijtewaal & Oliemans (1996); Kuerten (2006); Marchioli *et al.* (2003, 2008).

In flows with locally higher mass loading, two-way coupling effects may become important. In addition to solving the particle dynamics, a two-way coupling point-particle algorithm must impose a localized momentum source/sink corresponding to the particle back-reaction to the flow. The classical approach is the particle-in-cell (PIC) method, developed by Crowe *et al.* (1977). Although widely used, the success of this method strongly depends on the number of particles per grid cell, i.e. it does not converge with grid refinement. Approaches for a consistent and more robust treatment are the object of active research, as shown by the number of recent studies, e.g. Gualtieri *et al.* (2015); Horwitz & Mani (2016); Ireland & Desjardins (2017). Investigations of particle-laden turbulent flows in the two-way coupling regime are found in Vreman *et al.* (2009); Capecelatro *et al.* (2018).

Despite the numerous studies involving DNS with point-particle methods, validations of the underlying assumptions remain scarce, even for simple flows. For instance, the parameter range where the Maxey-Riley-Gatignol equations are valid remains elusive (Bergougnoux *et al.* 2014). Though experiments in particle-laden turbulence are insightful (Eaton & Fessler 1994; Kaftori *et al.* 1995), parameter-matched numerical simulations remain challenging, because of the numerical limitations in terms of Reynolds number and the need for experiments in well-controlled, often idealised, configurations. Another possible reference for new models is a particle-resolved DNS, i.e. a DNS that resolves the flow around the surface of each small particle. Despite the great computational challenge of such computations, the first direct comparisons between point-particle models and particle-resolved simulations have started to appear for decaying homogeneous isotropic turbulence (HIT) (Schneiders *et al.* 2017; Mehrabadi *et al.* 2018).

We consider particle-laden turbulent channel flow, a widely-studied case with minimal governing parameters and particularly important to benchmark models for wall-bounded particle transport. Though interface-resolved DNS of these flows are in general quite demanding, recent studies have demonstrated that massively-parallel simulations of wall-bounded flows with $O(10^6)$ interface-resolved particles and $O(10^9 - 10^{10})$ grid points have become feasible (see Costa *et al.* 2016; Kidanemariam & Uhlmann 2017).

We present interface-resolved DNS of gravity-free turbulent channel flow laden with small inertial particles (with a size of 3 viscous units, and 100 times denser than the fluid), in the dilute regime. Two cases are considered, with bulk volume solid fractions that approach the one-way coupling regime: 0.003% and 0.03%. These cases are complemented with the corresponding one-way coupling point-particle DNS at the same Reynolds number. All cases show the expected turbophoretic particle drift towards the wall, but

Case	Φ (N_p)	Ψ	Notes	Re_τ
VD	0.003% (500)	0.337%	interface-resolved (VD)	179
D	0.034% (5 000)	3.367%	interface-resolved (D)	190
PP	—	—	point-particle (1-way coupling)	179

TABLE 1. Computational parameters of the DNS dataset. Φ/Ψ denotes the bulk solid volume/mass fraction, and N_p the total number of particles. For all cases, the bulk Reynolds number $Re_b = 5600$ (i.e. unladen friction Reynolds number $Re_\tau^{sph} \approx 180$); particle size ratio $D/(2h) = 1/120$; particle-to-fluid mass density ratio $\Pi_\rho = 100$, corresponding to a particle diameter (in viscous units) $D^+ = 3$ and a Stokes number $St = 50$. For the interface-resolved cases, the fluid domain is discretized on a regular Cartesian grid with $(L_x/N_x) \times (L_y/N_y) \times (L_z/N_z) = (6h/4320) \times (3h/2160) \times (2h/1440)$, while the particles are resolved with $D/\Delta x = 12$ grid points over the particle diameter (420 Lagrangian grid points in total). For case *PP*, the grid is 8 times coarser in each direction. Note that the last column reports the friction Reynolds number Re_τ extracted from the simulations.

the concentration profiles differ: resolved particles show a factor 2 – 3 smaller near-wall concentration. Because of the inhomogeneous particle distribution, non-negligible two-way coupling effects are found for the case with the largest volume fraction, but not in the most dilute case. The latter case is therefore used as reference for the one-way coupling regime, to show that the widely-used one-way coupling point-particle approach cannot accurately predict the near-wall particle dynamics, as it does not model short-range particle-wall interactions responsible for a much faster particle-wall detachment.

2. Methods and Computational Setup

The Navier-Stokes equations governing the fluid phase are solved with a second-order finite-difference method on a three-dimensional, staggered Cartesian grid, using a FFT-based pressure-projection method (Kim & Moin 1985). The solver was extended with a direct forcing immersed-boundary method (IBM) for particle-laden flows developed by Breugem (2012) and the lubrication/soft-sphere collision model for short-range particle-particle and particle-wall interactions in Costa *et al.* (2015). Several recent studies describe the method, present validations, and access its computational performance (Picano *et al.* 2015; Costa 2018; de Motta *et al.* 2019).

The particles are considered rigid, spherical and frictionless, with a normal dry coefficient of restitution $e_{n,d} = 0.97$. The domain is periodic in the streamwise (x) and spanwise (z) directions, with no-slip/no-penetration boundary conditions imposed at the walls ($y = h \mp h$), where h is the channel half height. The flow is driven by a uniform pressure gradient that ensures a constant bulk velocity. The physical and computational parameters are reported in table 1. Since the IBM requires a fixed, regular Eulerian grid, resolving the particles with $O(10)$ grid points over the diameter is, by far, what dictates the grid resolution. Hence, the spatial resolution for the interface-resolved simulations is, in each direction, about one order of magnitude larger than what is required for single-phase simulation, leading to $\sim 10^{10}$ grid points.

To mimic a flow close to the one-way coupling regime, we consider two low values of solid volume fraction, $\Phi \simeq 3 \cdot 10^{-6}$, denoted very dilute (VD), and $\Phi \simeq 3 \cdot 10^{-5}$, dilute (D). The bulk Reynolds number $Re_b \equiv U_b(2h)/\nu = 5600$, which corresponds to an unladen friction Reynolds number $Re_\tau^{sph} \equiv u_\tau h/\nu = 180$; U_b is the flow bulk velocity, u_τ the wall friction velocity, and ν the fluid kinematic viscosity. The particle properties are chosen close to those used in point-particle simulations at the same Re_τ ,

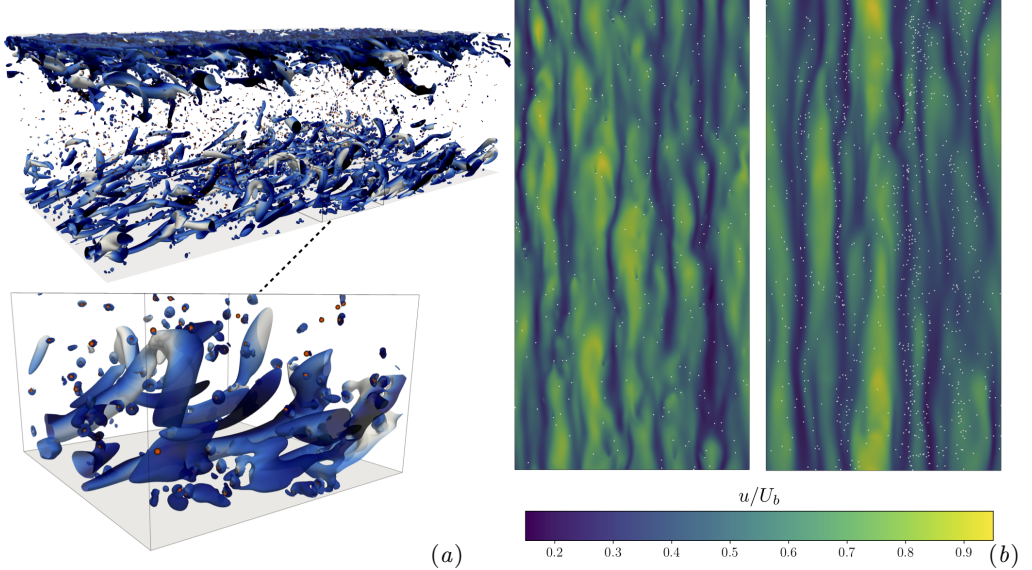


FIGURE 1. (a) Visualization of case *D*. Isocontours of the Q-criterion $Q = 20(U_b/h)^2$ colored by the local wall-normal velocity v . The interface-resolved particles are depicted in orange color. (b) Contours of streamwise velocity (flow from bottom to top) in the plane $y/h = 0.014$, i.e. $y^+ \approx 10$. Particles with wall distance $y_p/h < 0.015$ are depicted in white color.

which result in strong turbophoresis and large-scale clustering (Sardina *et al.* 2012). This choice corresponds to a particle Reynolds number $Re_p \equiv Du_\tau/\nu = D^+ = 3$, and Stokes number $St_p \equiv \Pi_\rho Re_p^2/18 = 50$, where D is the particle diameter and Π_ρ the particle-to-fluid mass density ratio.

The interface-resolved simulations are complemented with a one-way point-particle simulation (PP). Given the large density ratio, we assume that the particle dynamics simplifies to a balance between inertial and non-linear (Schiller-Naumann) drag forces. For this reference case, the fluid velocity at the particle position is obtained with trilinear interpolation, and the particle positions integrated in time with the same third-order low-storage Runge-Kutta scheme used for the fluid phase. For particle-wall collisions, a perfectly-elastic hard-sphere rebound is adopted. Test simulations showed that the results are not sensitive to Faxén corrections in the particle dynamics.

3. Results

Figure 1(a) shows a visualization of the particle-laden flow for case *D*. Similarly to case *VD* (not shown), the near-wall large-scale structures resemble those of the unladen flow. Nonetheless, the localized effect of the particles is evident, as depicted by the high-vorticity trail due to their wakes. The overall drag is a measure of the cumulative effect of the localized disturbances: this is reported in the last column of table 1 in terms of a friction Reynolds number $Re_\tau \equiv u_\tau h/\nu$. While the very dilute (*VD*) case shows, as expected, the same drag as the unladen flow, the dilute case (*D*) shows about 5% higher friction Reynolds number (i.e. about 10% increase in pressure drop). This is a remarkable increase, since a volume fraction of the order of 10^{-5} , and mass fraction of order 10^{-2} are often assumed to be in the 1-way coupling regime. Note that a similar drag increase is observed for finite-sized neutrally-buoyant particle suspensions with volume fraction of 5% (Picano *et al.* 2015). The modulation of the near-wall structures for case *D* is

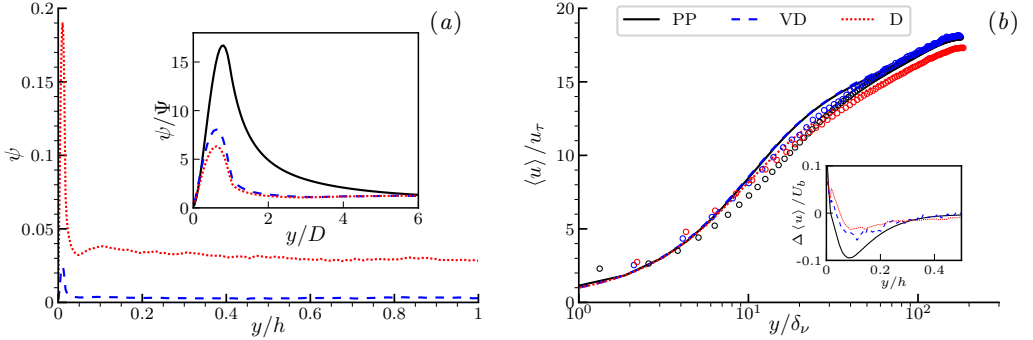


FIGURE 2. (a) Local solid mass fraction as a function of the outer-scaled wall-normal distance. The inset shows the corresponding bulk-normalized profile, versus the wall-distance in particle diameters. (b) Inner-scaled mean velocity profiles for the different cases (lines – fluid velocity; symbols – particle velocity). The inset shows the outer-scaled difference between fluid and particle velocity profiles $\Delta \langle u \rangle$.

noticeable in panel (b) of figure 1, where we display the streamwise velocity contours close to the wall. In addition to showing a microscopic footprint, the resolved particles disrupt streamwise-correlated near-wall structures. We will see that these observations are closely connected to the inhomogeneous particle distribution near the wall.

Figure 2(a) depicts the wall-normal profiles of the local solid mass fraction as a function of the wall-normal distance. The inset shows the same quantity divided by the bulk values versus the wall-normal distance in particle diameters. The profiles show a near-wall peak at $y \approx D/2$, about one order of magnitude larger than the bulk value, which explains the drag increase observed in case *D*. Despite the low bulk mass loading, the near-wall mass fraction becomes high enough to modulate the flow in this critical region ($\Psi \simeq 0.2$). We should note that the corresponding local volume fraction is still too low ($\Phi \simeq 0.002$) for particle-particle interactions to be significant: the collision frequency in the viscous sublayer is virtually zero. The interface-resolved simulations show pronounced differences when compared to the point-particle results (*PP*), with the latter over-predicting the concentration peak by a factor of 2 – 3. Moreover, the concentration profile of case *PP* shows a more gentle decrease away from the wall, while in the other cases the concentration peak corresponds to a single particle layer. At least for the very dilute case *VD*, these differences cannot be explained in terms of turbulence modulation nor particle-particle interactions (i.e. two-/four-way coupling effects). Hence, a different near-wall dynamics of (isolated) particles must be the cause.

Figure 2(b) shows the inner-scaled profiles of mean streamwise fluid and particle velocity for the different cases. While the fluid velocity profile of case *VD* matches that of the unladen flow, case *D* shows significant deviations. Since the outer-scaled profiles of all cases collapse in the outer region (not shown), these deviations are attributed to the increase in wall shear. We thus confirm that, somewhat unexpectedly, only case *VD* satisfies the 1-way coupling assumption, i.e. the dispersed phase does not modulate the turbulent flow. This case serves therefore as benchmark to assess the validity of the point-particle model to predict the dispersed-phase dynamics in the 1-way coupling regime.

As for the particles, they tend to flow slower than the fluid in the buffer layer ($10 \lesssim y/\delta_\nu \lesssim 40 - 50$; see also the figure inset, showing the outer-scaled difference between the profiles of each phase). This velocity difference is more pronounced in case *PP*, where the particle velocity reduction is clear also very close to the wall. This has been observed in previous studies using point-particle DNS (Sardina *et al.* 2012), and is attributed to the

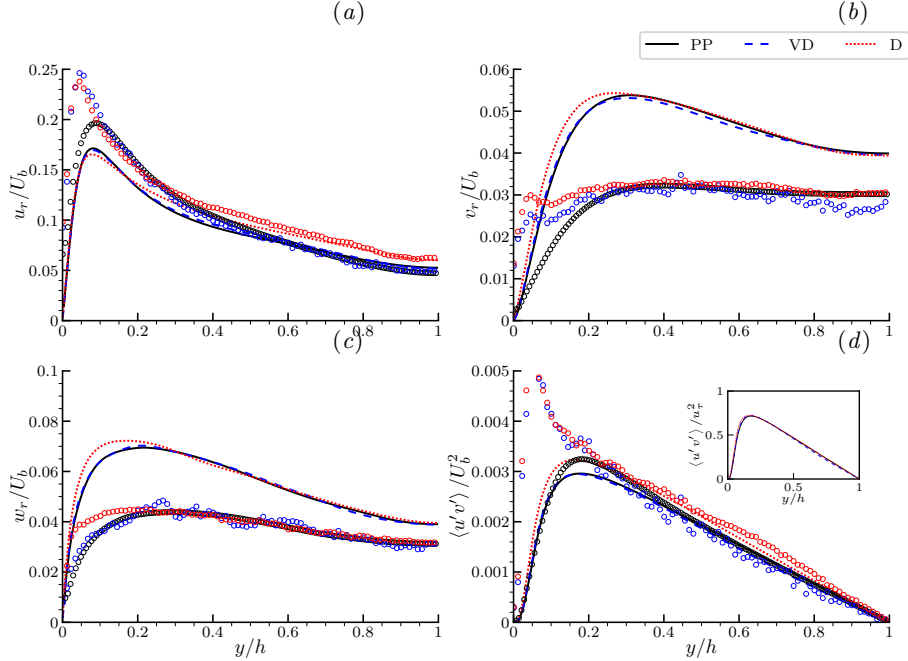


FIGURE 3. Outer-scaled second-order moments of particle velocity. (a) streamwise velocity r.m.s. (b) wall-normal velocity r.m.s. (c) ditto for spanwise velocity. (d) Reynolds stresses profile with inner-scaled inset. Lines – fluid; symbols – particles.

preferential sampling of the fluid low-speed streaks near the wall. The particle-resolved cases show a much weaker reduction of the mean particle velocity, which suggests that particles reside in the low-speed regions for shorter periods before re-suspending into the bulk, see also the discussion below about the particle dynamics. In the viscous sublayer, particles show a slightly higher mean velocity in the interface-resolved simulations. This higher slip velocity causes *hot-spots* of higher wall shear stress, which favor an increase in overall drag (Costa *et al.* 2016, 2018). Clearly this effect is significant in case *D*, where the near-wall number density is high enough, but not in case *VD*.

Figure 3 shows the second-order statistics of fluid and particle velocity. Focusing first on the fluid phase, we see once more that the data for *VD* tends to those of the single phase flow, whereas turbulence modulation is evident for case *D*. Here the Reynolds stresses are higher, consistently with the overall drag increase (see inset). Moreover, small differences are found for all the velocity r.m.s. of case *D* near the wall, where the velocity fluctuations become less anisotropic, i.e. u_r decreases and v_r and w_r increase. This is attributed to the enhanced mixing due to the near-wall particles, whose local mass fraction is high enough for 2-way coupling effects to be significant.

Remarkably, the second-order moments of the particle velocity for the fully-resolved one-way coupling case, *VD*, strongly differ from those of the point-particle simulations near the wall, while in the bulk the two cases display a similar behavior. In the bulk, where the local shear is relatively low, the point-particle model succeeds in predicting the particle dynamics. We should note that the same closure for the point-particle dynamics was used in Mehrabadi *et al.* (2018) for decaying HIT, and the results also compared well to the corresponding interface-resolved case. Closer to the wall ($y/h \lesssim 0.1$), however, the interface-resolved simulations show higher fluctuation levels than the point-

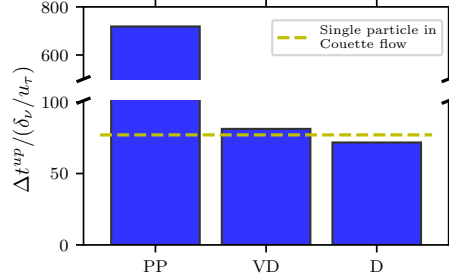


FIGURE 4. Inner-scaled average time a wall-skimming particle takes to reach a wall-normal distance $y > 5\delta_\nu$ (i.e. to exit the viscous sublayer), Δt^{up} . The dashed yellow line correspond to the time a wall-skimming particle takes, in a model laminar Couette flow at equivalent Reynolds number, to reach the same inner-scaled wall-normal distance.

particle reference. The exception is the spanwise velocity r.m.s. w_r , which attains similar values also close to the wall for case *VD* and *PP*. This suggests different single-particle dynamics, as particles approach and depart from the wall. We should note that similar results for the streamwise and wall-normal particle velocity r.m.s. have been observed in recent experiments of particle-laden turbulent downward flow in a vertical channel; see Fong *et al.* (2019). In the one-way point-particle DNS, the particle dynamics is modeled by a simple drag law, without considering short-range hydrodynamic particle-wall interactions. In this case, particles are driven towards the wall with high velocity by turbophoresis. Their inertia prevents resuspension, resulting in long periods of wall accumulation in low-speed regions, while only few of them drift back into the bulk (Soldati & Marchioli 2009; Sardina *et al.* 2012). Since at equilibrium the net wall-normal particle flux is zero, a large number of particles accumulate at the wall. Conversely, when the flow around particles is resolved, the short-range particle-wall hydrodynamic interactions alter the dynamics: particles tend to reside for much shorter times near the wall before re-suspending. Hence, point-particles tend to skim along the wall in low-speed streaks for long periods (Soldati & Marchioli 2009; Sardina *et al.* 2012) whereas resolved particles show shorter residence times at the wall, quickly take off, and are not preferentially localized in low-speed streaks, see figure 1(*b*). This faster cycle explains the larger value of v_r near the wall, and consequently the larger value of u_r and $\langle u'v' \rangle$ since the fluctuations are correlated through the mean shear. To better quantify this, figure 4 shows the average time that a particle close to the wall (i.e. located at $y \approx D_p/2$) needs to exit the viscous sublayer (i.e. to reach a wall-normal position $y > 5\delta_\nu$), Δt^{up} . The figure shows that near-wall particles in the fully-resolved cases take about the same time to exit the viscous sublayer, which is about one order of magnitude shorter than that of the point-particle DNS *PP*.

This particle dynamics suggest a missing key ingredient, absent in the point-particle model: a particle-wall hydrodynamic interaction combined with a shear-induced inertial lift force. Such a force plays a very important role in the particle dynamics near the wall, where the mean shear is high (Soldati & Marchioli 2009). It is known that a particle flowing near a wall in a shear flow experiences a strong lift force due to short-range particle-wall interactions (Cherukat & McLaughlin 1994). A similar mechanism should work for small particles in the viscous sublayer of a turbulent flow.

To better understand the mechanism for particle detachment, we performed an auxiliary DNS of laminar Couette flow at the same particle Reynolds number. The computational domain has size $L_x \times L_y \times L_z = 20D \times 10D \times 10D$ with a regular grid where

$D/\Delta x = 16$. The boundary conditions are the same as for the turbulent channel flow, except that the flow is now driven by a non-zero streamwise velocity U_w at $y = L_y$. The Reynolds number based on the local shear rate $\dot{\gamma} \equiv U_w/L_y$ and particle size is set to match that of the particle in the viscous sublayer, i.e. $\dot{\gamma}D^2/\nu = (u_\tau/\delta_v)D^2/\nu$. A single particle with the same physical properties is placed at the bottom wall, with initial linear and angular velocity conforming to the local flow velocity and vorticity. The flight time Δt^{up} for the particle to detach from the wall and travel 5 viscous units in y is reported by the dashed line of figure 4. The measured time is remarkably close to the average value measured in the interface-resolved DNS for the two turbulent cases under consideration. This strongly suggests that the mechanism for particle detachment from the wall is, to first approximation, purely shear-driven. It should be noted that in the current one-way point-particle model a particle placed at the wall in a laminar Couette flow would never detach from it. We conclude that this difference creates the strong discrepancies between the interface-resolved simulation in the very dilute regime and the results from the point-particle method, both in terms of wall accumulation and near-wall particle velocity statistics.

We have seen that the dynamics of resolved and point-particles are similar in the bulk, and thus the drift towards the wall is well described by point-particle methods. When moving along the wall, particle-wall interactions induce strong lift forces that quickly dislodge resolved particles. This mechanism is absent in current point-particle models, which instead display slow resuspension and particles spending long time in the near-wall low-speed streaks. This enhances the prediction of turbophoretic wall accumulation in point-particle simulations.

4. Conclusions

We have presented a direct comparison between point-particle and particle-resolved DNS of turbulent channel flow laden small inertial particles. Two particle-resolved cases have been considered, with volume fractions of $3 \cdot 10^{-4}$ and $3 \cdot 10^{-5}$, with only the latter case falling into the one-way coupling assumption, i.e. the particles do not influence the statistics of the turbulence. The less dilute case, instead, shows about 10% drag increase compared to the unladen case. This striking increase is attributed to a significant particle mass fraction near the wall caused by turbophoresis. These particles flow with high particle-to-fluid (apparent) slip velocity, producing *hot spots* of large wall shear.

We then examine the differences between the most dilute case, which satisfies the one-way coupling assumption, and a classic one-way point-particle simulation where the particle acceleration is balanced by the non-linear (Schiller-Naumann) drag. While in the bulk of the channel concentration profiles and moments of the particle velocity agree well, most of these quantities show clear differences close to the wall. This disagreement is attributed to a missing key ingredient in the point-particle simulation: a lift force due to the combination of short-range particle-wall interactions and local shear rate. To test this hypothesis, the average particle residence time in the viscous sublayer has been measured and compared to that of a single resolved sphere in a laminar Couette flow with matched (particle shear) Reynolds number. The average flight time of the resolved particles in turbulent channel is extremely close to that of the laminar simulation, strongly supporting our interpretation. Conversely, point-particles reside in the viscous sublayer for a time about one order of magnitude longer. Properly accounting for these near-wall dynamics is therefore fundamental to accurately predict the particle statistics without resolving the particles.

All differences between resolved and point-particle statistics can be related to this wall-

particle interaction. First, the high-concentration at the wall in the interface-resolved simulations is limited to a single particle layer, since particles tend to promptly depart from the wall. Second, particles are resuspended before they can accumulate for long time in low-speed streaks, which lowers the apparent slip velocity in the near-wall region. Finally, because of this wall-lift force, particles show higher near-wall velocity fluctuations.

We have shown that predicting the near-wall dynamics in a canonical channel flow with a standard point-particle model is not a trivial task. We hope that the present results can be exploited for the development of improved point-particle models for one- and two-way coupling in wall-bounded turbulent flows.

This work was supported by the European Research Council grant no. ERC-2013-CoG-616186, TRITOS. We acknowledge computer time provided by SNIC (Swedish National Infrastructure for Computing), and PRACE for awarding us access to the supercomputer Marconi, based in Italy at CINECA under project 2017174185 – DILPART.

REFERENCES

BALACHANDAR, S & EATON, JOHN K 2010 Turbulent dispersed multiphase flow. *Annual review of fluid mechanics* **42**, 111–133.

BERGOUGNOUX, LAURENCE, BOUCHET, GILLES, LOPEZ, DIEGO & GUAZZELLI, ELISABETH 2014 The motion of solid spherical particles falling in a cellular flow field at low stokes number. *Physics of Fluids* **26** (9), 093302.

BREUGEM, WIM-PAUL 2012 A second-order accurate immersed boundary method for fully resolved simulations of particle-laden flows. *Journal of Computational Physics* **231** (13), 4469–4498.

CAPECELATRO, JESSE, DESJARDINS, OLIVIER & FOX, RODNEY O 2018 On the transition between turbulence regimes in particle-laden channel flows. *Journal of Fluid Mechanics* **845**, 499–519.

CHERUKAT, PRADEEP & MC LAUGHLIN, JOHN B 1994 The inertial lift on a rigid sphere in a linear shear flow field near a flat wall. *Journal of Fluid Mechanics* **263**, 1–18.

COSTA, PEDRO 2018 A fft-based finite-difference solver for massively-parallel direct numerical simulations of turbulent flows. *Computers & Mathematics with Applications* **76** (8), 1853 – 1862.

COSTA, PEDRO, BOERSMA, BENDIKS JAN, WESTERWEEL, JERRY & BREUGEM, WIM-PAUL 2015 Collision model for fully resolved simulations of flows laden with finite-size particles. *Physical Review E* **92** (5), 053012.

COSTA, PEDRO, PICANO, FRANCESCO, BRANDT, LUCA & BREUGEM, WIM-PAUL 2016 Universal scaling laws for dense particle suspensions in turbulent wall-bounded flows. *Physical review letters* **117** (13), 134501.

COSTA, PEDRO, PICANO, FRANCESCO, BRANDT, LUCA & BREUGEM, WIM-PAUL 2018 Effects of the finite particle size in turbulent wall-bounded flows of dense suspensions. *Journal of fluid mechanics* **843**, 450–478.

CROWE, CLAYTON T, SHARMA, M PT & STOCK, DAVID E 1977 The particle-source-in cell (psi-cell) model for gas-droplet flows. *Journal of fluids engineering* **99** (2), 325–332.

EATON, JOHN K & FESSLER, JR 1994 Preferential concentration of particles by turbulence. *International Journal of Multiphase Flow* **20**, 169–209.

ELGHOBASHI, SAID 1994 On predicting particle-laden turbulent flows. *Applied scientific research* **52** (4), 309–329.

FESSLER, JOHN R, KULICK, JONATHAN D & EATON, JOHN K 1994 Preferential concentration of heavy particles in a turbulent channel flow. *Physics of Fluids* **6** (11), 3742–3749.

FONG, KEE ONN, AMILI, OMID & COLETTI, FILIPPO 2019 Velocity and spatial distribution of inertial particles in a turbulent channel flow. *arXiv preprint arXiv:1904.06381* .

GATIGNOL, RENÉE 1983 The faxén formulas for a rigid particle in an unsteady non-uniform stokes-flow. *Journal de Mécanique théorique et appliquée* **2** (2), 143–160.

GUALTIERI, PAOLO, PICANO, F, SARDINA, GAETANO & CACCIOLA, CARLO MASSIMO 2015 Exact regularized point particle method for multiphase flows in the two-way coupling regime. *Journal of Fluid Mechanics* **773**, 520–561.

HORWITZ, JAK & MANI, ALI 2016 Accurate calculation of stokes drag for point-particle tracking in two-way coupled flows. *Journal of Computational Physics* **318**, 85–109.

IRELAND, PETER J & DESJARDINS, OLIVIER 2017 Improving particle drag predictions in euler-lagrange simulations with two-way coupling. *Journal of Computational Physics* **338**, 405–430.

KAFTORI, D, HETSRONI, G & BANERJEE, S 1995 Particle behavior in the turbulent boundary layer. i. motion, deposition, and entrainment. *Physics of Fluids* **7** (5), 1095–1106.

KIDANEMARIAM, AMAN G & UHLMANN, MARKUS 2017 Formation of sediment patterns in channel flow: minimal unstable systems and their temporal evolution. *Journal of Fluid Mechanics* **818**, 716–743.

KIM, JOHN & MOIN, PARVIZ 1985 Application of a fractional-step method to incompressible navier-stokes equations. *Journal of computational physics* **59** (2), 308–323.

KUERTEN, JGM 2006 Subgrid modeling in particle-laden channel flow. *Physics of fluids* **18** (2), 025108.

MARCHIOLI, CRISTIAN, GIUSTI, ANDREA, SALVETTI, MARIA VITTORIA & SOLDATI, ALFREDO 2003 Direct numerical simulation of particle wall transfer and deposition in upward turbulent pipe flow. *International journal of Multiphase flow* **29** (6), 1017–1038.

MARCHIOLI, CH, SOLDATI, A, KUERTEN, JGM, ARGEN, B, TANIÈRE, A, GOLDENOPH, G, SQUIRES, KD, CARGNELUTTI, MF & PORTELA, LM 2008 Statistics of particle dispersion in direct numerical simulations of wall-bounded turbulence: Results of an international collaborative benchmark test. *International Journal of Multiphase Flow* **34** (9), 879–893.

MAXEY, MARTIN R & RILEY, JAMES J 1983 Equation of motion for a small rigid sphere in a nonuniform flow. *The Physics of Fluids* **26** (4), 883–889.

MEHRABADI, M, HORWITZ, JAK, SUBRAMANIAM, S & MANI, A 2018 A direct comparison of particle-resolved and point-particle methods in decaying turbulence. *Journal of Fluid Mechanics* **850**, 336–369.

DE MOTTA, JC BRÄNDLE, COSTA, P, DERKSEN, JJ, PENG, C, WANG, L-P, BREUGEM, W-P, ESTIVALEZES, JL, VINCENT, S, CLIMENT, E, FEDE, P & OTHERS 2019 Assessment of numerical methods for fully resolved simulations of particle-laden turbulent flows. *Computers & Fluids* **179**, 1–14.

PICANO, FRANCESCO, BREUGEM, WIM-PAUL & BRANDT, LUCA 2015 Turbulent channel flow of dense suspensions of neutrally buoyant spheres. *Journal of Fluid Mechanics* **764**, 463–487.

REEKS, MW 1983 The transport of discrete particles in inhomogeneous turbulence. *Journal of aerosol science* **14** (6), 729–739.

SARDINA, G, SCHLATTER, PHILIPP, BRANDT, LUCA, PICANO, F & CACCIOLA, CARLO MASSIMO 2012 Wall accumulation and spatial localization in particle-laden wall flows. *Journal of Fluid Mechanics* **699**, 50–78.

SCHNEIDERS, LENNART, MEINKE, MATTHIAS & SCHRÖDER, WOLFGANG 2017 On the accuracy of lagrangian point-mass models for heavy non-spherical particles in isotropic turbulence. *Fuel* **201**, 2–14.

SOLDATI, ALFREDO & MARCHIOLI, CRISTIAN 2009 Physics and modelling of turbulent particle deposition and entrainment: Review of a systematic study. *International Journal of Multiphase Flow* **35** (9), 827–839.

TOSCHI, FEDERICO & BODENSCHATZ, EBERHARD 2009 Lagrangian properties of particles in turbulence. *Annual review of fluid mechanics* **41**, 375–404.

UIJTTEWAAL, WSJ & OLIEMANS, RVA 1996 Particle dispersion and deposition in direct numerical and large eddy simulations of vertical pipe flows. *Physics of Fluids* **8** (10), 2590–2604.

VREMAN, BERT, GEURTS, BERNARD J, DEEN, NG, KUIPERS, JAM & KUERTEN, JOHANNES GM 2009 Two-and four-way coupled euler-lagrange large-eddy simulation of turbulent particle-laden channel flow. *Flow, turbulence and combustion* **82** (1), 47–71.